

REPORT DOCUMENTATION PAGE

Form Approved
OMB No. 0704-0188

Public reporting burden for this collection of information is estimated to average 1 hour per response, including the time for reviewing instructions, searching existing data sources, gathering and maintaining the data needed, and completing and reviewing this collection of information. Send comments regarding this burden estimate or any other aspect of this collection of information, including suggestions for reducing this burden to Department of Defense, Washington Headquarters Services, Directorate for Information Operations and Reports (0704-0188), 1215 Jefferson Davis Highway, Suite 1204, Arlington, VA 22202-4302. Respondents should be aware that notwithstanding any other provision of law, no person shall be subject to any penalty for failing to comply with a collection of information if it does not display a currently valid OMB control number. PLEASE DO NOT RETURN YOUR FORM TO THE ABOVE ADDRESS.

1. REPORT DATE (DD-MM-YYYY)		2. REPORT TYPE Technical Paper		3. DATES COVERED (From - To)	
<div style="border: 1px solid black; border-radius: 50%; padding: 20px; text-align: center; width: fit-content; margin: 0 auto;"> Please see attached </div>				4. TITLE AND SUBTITLE	
				5a. CONTRACT NUMBER F04611-98-C-0010	
				5b. GRANT NUMBER	
				5c. PROGRAM ELEMENT NUMBER 62203F	
				5d. PROJECT NUMBER 1011	
6. AUTHOR(S)				5e. TASK NUMBER 00NM	
				5f. WORK UNIT NUMBER 346281	
7. PERFORMING ORGANIZATION NAME(S) AND ADDRESS(ES) ORBITEC				8. PERFORMING ORGANIZATION REPORT	
9. SPONSORING / MONITORING AGENCY NAME(S) AND ADDRESS(ES) Air Force Research Laboratory (AFMC) AFRL/PRS 5 Pollux Drive Edwards AFB CA 93524-7048				10. SPONSOR/MONITOR'S ACRONYM(S)	
				11. SPONSOR/MONITOR'S NUMBER(S) AFRL-PR-ED-TP-1998-158	
12. DISTRIBUTION / AVAILABILITY STATEMENT Approved for public release; distribution unlimited.					
13. SUPPLEMENTARY NOTES					
14. ABSTRACT <div style="text-align: right; font-size: 2em; font-weight: bold;">20030310 097</div>					
15. SUBJECT TERMS					
16. SECURITY CLASSIFICATION OF:			17. LIMITATION OF ABSTRACT A	18. NUMBER OF PAGES	19a. NAME OF RESPONSIBLE PERSON Leilani Richardson
a. REPORT Unclassified	b. ABSTRACT Unclassified	c. THIS PAGE Unclassified			19b. TELEPHONE NUMBER (include area code) (661) 275-5015



AIAA 98-3508

**Advanced Cryogenic Solid Hybrid Rocket
Engine Developments: Concept and Testing**

C. St.Clair, E. Rice, W. Knuth, and D. Gramer
Orbital Technologies Corporation (ORBITEC™)
Madison, WI

**34th AIAA/ASME/SAE/ASEE
Joint Propulsion Conference & Exhibit
July 13-15, 1998 / Cleveland, OH**

ADVANCED CRYOGENIC SOLID HYBRID ROCKET ENGINE DEVELOPMENTS: CONCEPT AND TEST RESULTS

Christopher P. St.Clair*, Eric E. Rice†, William H. Knuth‡, and Daniel J. Gramer§
Orbital Technologies Corporation (ORBITEC™)

Abstract

ORBITEC has conducted considerable R&D under various USAF and NASA contracts and company sponsored efforts to develop a new class of rocket propulsion devices, cryogenic solid rocket engines. The basic concept of these engines is to freeze a propellant which is normally a gas at room temperature into a solid propellant grain. This solid grain is then combusted with a second propellant. These rocket engines promise a number of advantages over conventional liquid rocket engines, including increased simplicity, safety, propellant density, and potentially performance with the addition of High-Energy Density Matter (HEDM's). ORBITEC has tested cryogenic solid hybrid rocket engines including the following propellant combinations: (1) solid oxygen/gaseous hydrogen; (2) solid hydrogen/gaseous oxygen; (3) solid methane/gaseous oxygen; and (4) solid methane-aluminum/gaseous oxygen. The primary focus of this paper is on solid oxygen/gaseous hydrogen. Work achieved to date includes: (1) a total of over 50 solid oxygen test firings; (2) establishment of regression rate data for the different propellant combinations, where the rates can be a factor of 20 to 40 times higher than conventional HTPB-based hybrids; (3) achievement of burn durations from 1 to 30 seconds; and (4) engine chamber pressures as high as 250 psi. The potential applications include: research devices to test high-energy density matter (HEDM); hybrid rocket launch vehicle upper stages; or orbit transfer vehicles. During a current sponsored USAF Research Laboratory (RL, Edwards Air Force Base, CA) project, ORBITEC is to design, develop and test a larger, SOX/LH₂ flight-type engine that will have throttling and O/F ratio control.

History of the Cryogenic Hybrid

Orbital Technologies Corporation (ORBITEC™) first proposed cryogenic solid hybrid rocket engine applications to

the USAF/RL in 1991-1992 to support the HEDM Program. ORBITEC has had numerous contracts in this technology area under USAF/RL and NASA funding. The key thrust area has been to conduct cryogenic solid oxidizer and fuel formation research, supporting analysis, and designing, developing, testing, and demonstrating engines in support of hybrid rocket engine developments for HEDM and non-HEDM propulsion applications. Solid cryogens have included oxygen, hydrogen, and methane. ORBITEC has successfully first fired the following solid cryogen systems on the dates indicated below:

SOX/GH₂ Hybrid Rocket -- August 21, 1995
SCH₄/GO₂ Hybrid Rocket -- October 10, 1995
SH₂/GO₂ Hybrid Rocket -- October 25, 1996
SCH₄-AL/GO₂ Hybrid Rocket -- November 9, 1996.

Baseline Design

The basic design approach for the cryogenic solid hybrid engines is depicted in Figure 1. The engine is encased in a vacuum chamber to provide thermal insulation from ambient temperatures. A coolant (LHe or LN₂) fills the outer engine dewar. The coolant chills the wall of the center tube where the propellant is desired on the inner volume. The propellant gas is then admitted to the central chamber below its triple point pressure, and it begins to deposit directly from the gas phase on the chilled surface, slowly building up over time to form the solid grain. When the engine is ready to fire, the inner chamber is pressurized to one atmosphere with GHe, and then an ignitor flame enters from the head end. The gaseous component of the propellant combination is then injected at the top of the grain. The firing begins and the grain is depleted over time, producing combustion products which are expelled through the nozzle. Figure 2 shows the side view of the Mark-II system located in ORBITEC's test facility; the vacuum chamber is visible on the test stand.

* Member AIAA

† Associate Fellow AIAA

‡ Senior Member AIAA

§ Member AIAA

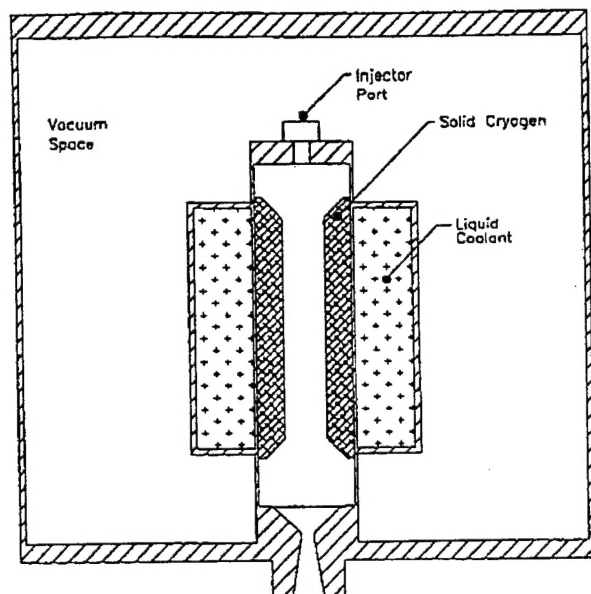


Figure 1. Engine Concept Design Sketch

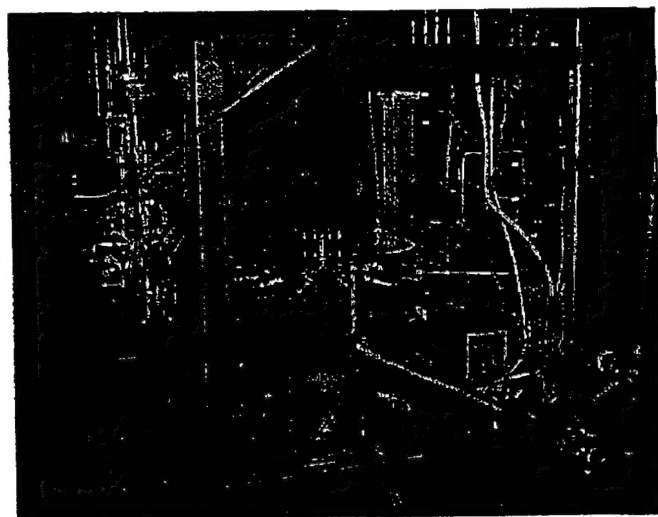


Figure 2. ORBITEC's Mark-II Cryogenic Hybrid Engine

Motivation for the Cryogenic Hybrid

Cryogenic hybrids offer a number of possible advantages over conventional engine systems:

- High performance. Theoretical values of specific impulse are only slightly lower than for liquid-liquid rocket engines, and substantially higher than for solid rocket motors and conventional hybrid engines.
- Increased density. Freezing one of the propellants can yield substantial density gains over liquid rocket engines. For example, solid hydrogen at 4 K has a density of 0.087 g/cc, as compared to 0.070 g/cc for liquid hydrogen at the normal boiling point; a gain of nearly 25%. Solid oxygen undergoes a 35% densification.
- Increased safety. Hybrid rocket engines inherently offer a degree of safety from catastrophic failures which is not available with liquid rocket engines or solid motors.
- Greater simplicity. With only one working fluid, hybrid engines are less complicated than liquid rocket engines.
- High regression rates. Regression rates from 20-40 times faster than those for conventional propellants have been measured. High regression rates are generally desirable in hybrid rockets to meet desired thrust levels and burn times. Conventional hybrids typically require wagon-wheel type fuel grains to obtain required propellant flow rates.
- HEDM potential. Solid propellant grains cooled to low cryogenic temperatures (<20 K) offer an ideal matrix for various high-energy density matter (HEDM) additives. Possibilities include ozone, atomic metals, and others.

Early Solid Oxygen Test Firing Results

Due to the large number of solid oxygen test firings performed to date (over 50 by ORBITEC), results will only be presented from selected firings. Figure 3 presents a summary of statistics from selected firings, including all firings discussed in this paper.

Firing #	Date	O ₂ Mass (g)	H ₂ Mass Flow (g/s)	Max. Steady Chamber Pressure (psia)	Burn Duration (sec)	Average O/F Ratio	Notes
G20-H010	21 Sep 95	250	1.5	190	8	21	Largest SOX grain to date; prototype engine.
G53-H010	21 Feb 97	150	4.2	120	6	6	Dual injection.
G60-P012	4 Feb 98	150	3.0	110	5	11	All head-end injection.
G60-P013	5 Feb 98	150	6.0	170	5	5	All head-end injection.
G60-P015	17 Apr 98	150	3.0	120	3	19	Warm grain test.
G60-P018	29 Apr 98	150	7.5	170	4	4	All head end-injection. Incomplete burn.
G60-P020	6 May 98	150	6.0	130	6	4	All head-end injection.
G60-P021	7 May 98	100	6 +/- 2	140	5	4	All head-end injection, pre-set flow profile.
G60-P023	21 May 98	150	2.1	170	9	8	Dual injection, dynamic flow control.

Figure 3. Summary Statistics for Selected SOX Test Firings

Figure 4 presents a pressure plot from test firing G20-H010, the final test firing performed in the initial prototype SOX engine¹. This firing exhibits a number of characteristics of the early tests. Despite the fact that the main hydrogen flow is at a maximum level by time=414 seconds, the chamber pressure continues to rise until nearly two seconds later. This start transient may be the result of warming either the grain or cold engine surfaces exposed to the combustion chamber. A long increasing transient of this type is typical of most of the solid oxygen tests performed to date, and remains an issue facing the current effort to achieve test firings with a constant chamber pressure.

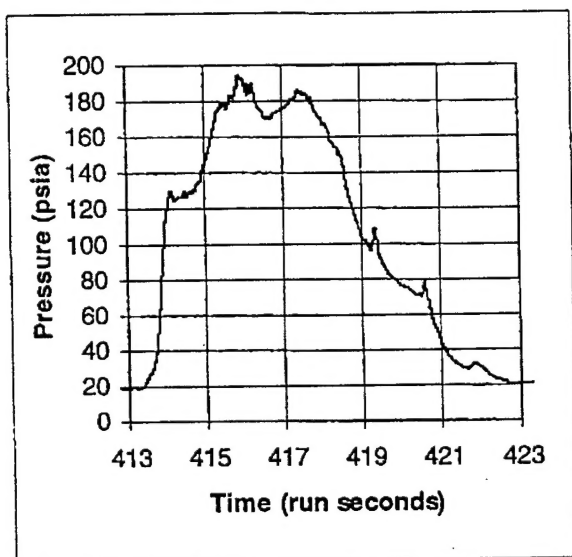


Figure 4. Pressure Trace for G20-H010

Figure 4 also exhibits a number of small pressure spikes. These have been associated with instability and partial breakup of the solid oxygen grain: as pieces of the grain break free and enter the gas stream, they momentarily deliver more oxygen into the combustion process. They may also cause partial blockages of the nozzle.

The first series of firings in the prototype engine was marked by extremely high O/F ratios: average values ranged from 11 to 46. This was a result of the unexpectedly high regression rates of the solid oxygen grains and the limitations of the gaseous hydrogen flow system that was in use at that time.

O/F Ratio Control Tests

Several techniques have been explored to control the O/F ratio resulting from SOX/hydrogen combustion. The most promising employs hydrogen injection at two locations. A small pilot flow of hydrogen is injected at the head end of the grain chamber. This burns with the oxygen coming off the oxygen grain, producing extremely oxygen-rich combustion

products. Desirable O/F ratios are around 150, producing a hot oxygen/steam mixture at approximately 550 K (530 F). Through controlling this flow, the oxygen regression rate (and hence the overall chamber pressure) may be controlled to some degree, providing a throttling capability. The main hydrogen flow is injected into an aft combustion chamber, where it burns with the oxygen-rich combustion gases entering from the grain chamber to trim the overall ratio to an optimum value. This injection approach also has the potential of achieving very high C* efficiency, because the aft injector may be designed to provide excellent mixing. Figure 5 shows a schematic of this dual-injection arrangement.

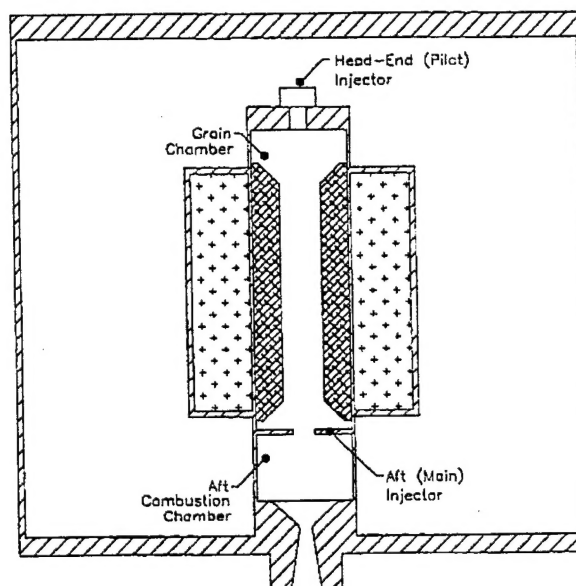


Figure 5. Head-end/Aft-end Injection Schematic

Early attempts at using tail-end injection to trim the O/F ratio to near 6 were successful in achieving the desired average O/F ratio over the entire firing. However, the chamber pressure underwent such a wide variation during the course of the firing that the instantaneous values of O/F ratio varied substantially, despite a constant hydrogen mass flow. Figure 6 shows the pressure trace for test firing G53-H010². The average O/F ratio for this test was 6.3, but estimated instantaneous values range from 2.5 at the beginning and end to 9.0 at the height of the firing.

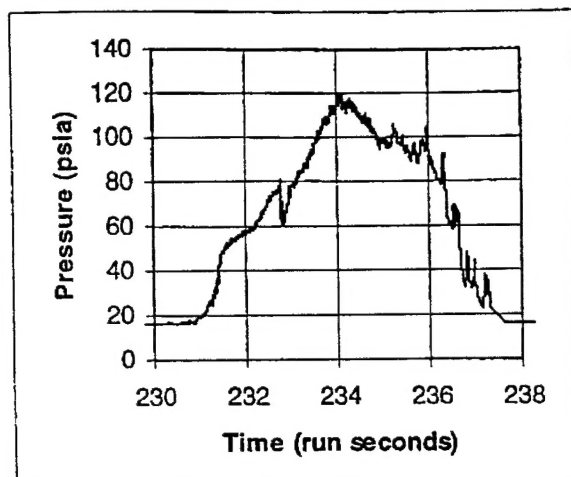


Figure 6. Pressure Trace for G53-H010

High Hydrogen Flow Tests

Another option for bringing the engine O/F ratio to the desired level is to simply increase the hydrogen mass flow into the grain chamber. As the hydrogen mass flux is increased, the oxidizer flow increases as well, but the overall O/F ratio decreases. This approach does not offer simultaneous control of both O/F ratio and chamber pressure, but it is simpler than the dual-injection arrangement.

The engine system was recently fitted with new hydrogen flow control equipment which allowed for higher flow rates. Figure 7 shows pressure traces from two of the resulting firings performed in February 1998 with varying hydrogen mass flow rates (3.0 and 6.0 g/s, respectively). Note the long tail-off associated with G60-P013. This is attributed to partial grain break-up.

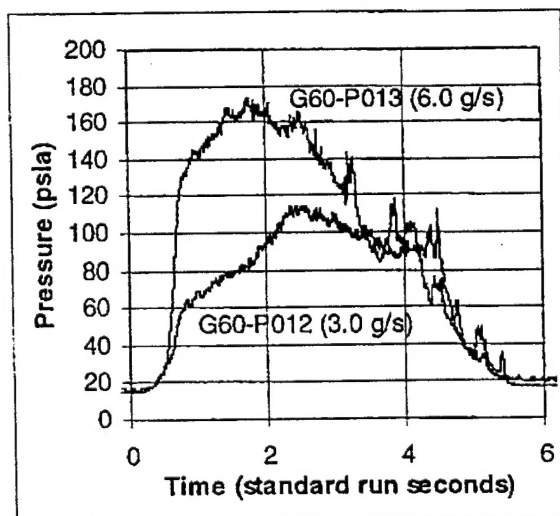


Figure 7. Pressure Traces for G60-P012 and G60-P013

Pressure traces for two more high-flow test firings are presented in Figure 8. Note the relatively flat trace observed in G60-P020; the grain for this test firing was formed using new measures intended to make it as uniform as possible. Grain optimization and the problem of grain break-up are discussed later in this paper.

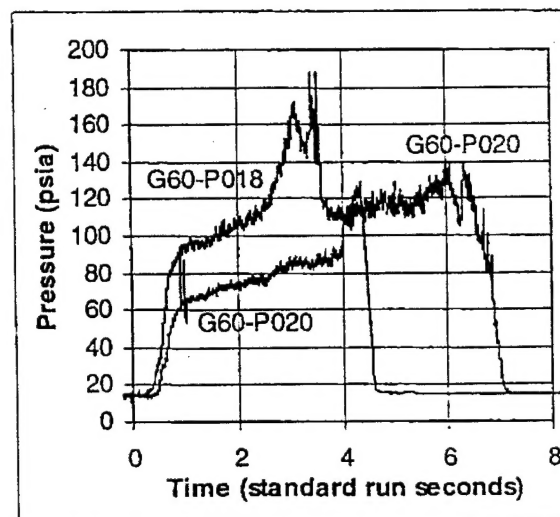


Figure 8. Pressure Traces for G60-P018 and G60-P020

Figure 9 shows the nozzle plume at the height of G60-P018. The heat-sink copper nozzle is visible at top center. The O/F ratio in Figure 9 is estimated at 6.

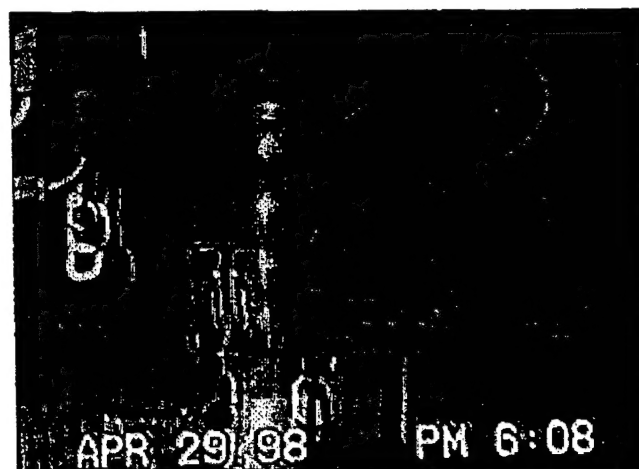


Figure 9. Nozzle Plume during G60-P018

Chamber Pressure Control Tests

The most recent tests have been dedicated to demonstrating active control of chamber pressure and O/F ratio. Test firing G60-P021 was performed with a pre-set hydrogen flow profile which brought the hydrogen flow up to 6 g/s, down to 4, up to 8, and back down to 6 again. Figure 10 shows the response of chamber pressure superimposed on the hydrogen

mass flow as a function of time. The chamber pressure tracks closely with the hydrogen mass flow rate, and also increases independent of hydrogen flow for the duration of the test firing.

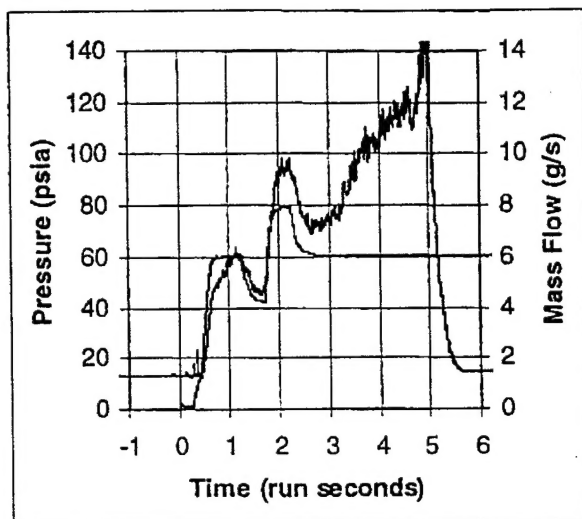


Figure 10. Chamber Pressure & Hydrogen Mass Flow for G60-P021

The tests following G60-P021 sought to use dual injection to control the chamber pressure and to maintain the O/F ratio near 6. To do this, a target pressure was established, and control logic was set up in the control program to vary the pilot flow to seek that target pressure. The main flow was adjusted along with the pilot flow to maintain a constant total flow of hydrogen into the system. In test firing G60-P023, the target was to hold the chamber pressure steady at 120 psi for approximately 8 seconds. Figure 11 shows the results, superimposing the chamber pressure with the pilot hydrogen supply pressure (proportional to the pilot hydrogen mass flow).

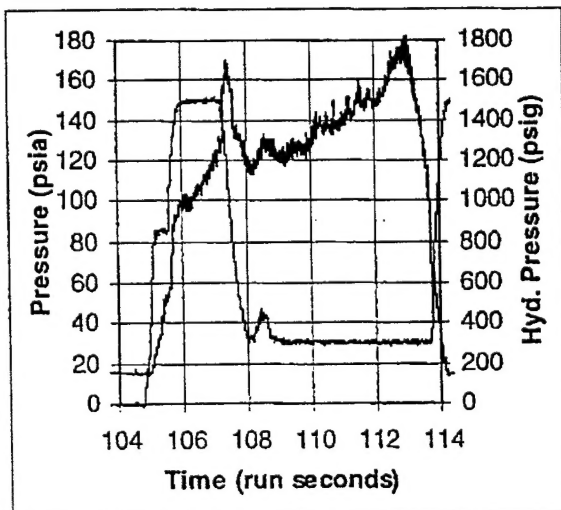


Figure 11. Chamber Pressure, Pilot Hydrogen Supply Pressure for G60-P023

A close study of Figure 11 shows the response of chamber pressure to changes in the hydrogen pilot flow. As the chamber pressure climbs past the target pressure of 120 psi, the pilot flow is reduced. This results in a decrease of chamber pressure, overshooting slightly below 120 psi. The controller damps the response, stabilizing around 120 psi. Unfortunately, the pilot flow then at its minimum level and the chamber pressure continues to climb, exhibiting the limitations of the control system.

Grain Uniformity & Stability Issues

Most of the pressure spikes and instabilities seen in the solid oxygen data are attributed to partial grain break-up. Solid methane offers an instructive comparison; Figure 12 shows pressure plots from three solid methane firings in which the oxygen mass flow rate was varied³. Observe the flat, steady pressure traces; these are characteristic of all solid methane tests performed by ORBITEC.

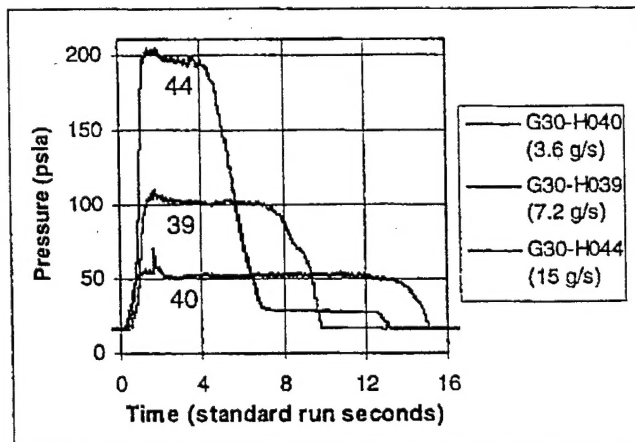


Figure 12. Effect of Oxygen Flow Rate on Pressure Profile, Selected Solid Methane Test Firings

Clearly, it is possible to freeze cryogenic grains which will burn evenly and smoothly. What, then, is the difference between the methane tests and the oxygen test firings? Several major possibilities have been identified and tested:

- 1) Grain cracking as a result of solid oxygen phase transformations; and
- 2) Grain non-uniformities caused by uneven heating of the grain surface, either during grain formation or early in the firing sequence.

One possibility has to do with the phase transformations undergone by solid oxygen between the melting point (54 K) and liquid helium temperatures. Three distinct phases exist, with phase transitions at 44 K and 24 K. Between 20 K and 54 K, SOX undergoes a density change of 14%, with 40% of this occurring at the upper phase transformation. This abrupt

density change could cause cracking and spalling of the grain as it is rapidly warmed during the firing.

To test this theory, a test was conducted in which it was attempted to warm the grain to approximately 51 K after forming it, then perform the firing. The pressure trace from this test is shown in Figure 13.

As Figure 13 shows, the test was not successful in achieving a flat pressure trace. In addition, the test was marked by rapid melting of the grain immediately prior to the firing and extremely poor C* efficiency (55%, as compared to normal values around 80%). Figure 14 shows a view of the nozzle approximately 1.3 seconds after the vacuum in the grain chamber is broken with a helium purge. The large plate in the bottom of the view is in the process of swinging open to clear the nozzle. Note the droplets of liquid oxygen streaming out of the nozzle.

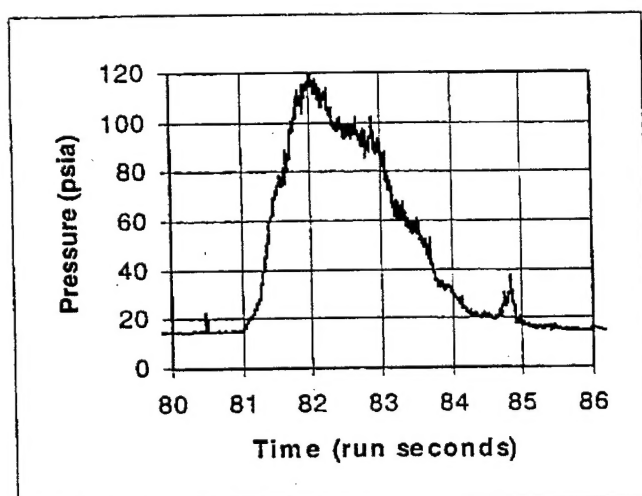


Figure 13. Pressure Trace for G60-P015

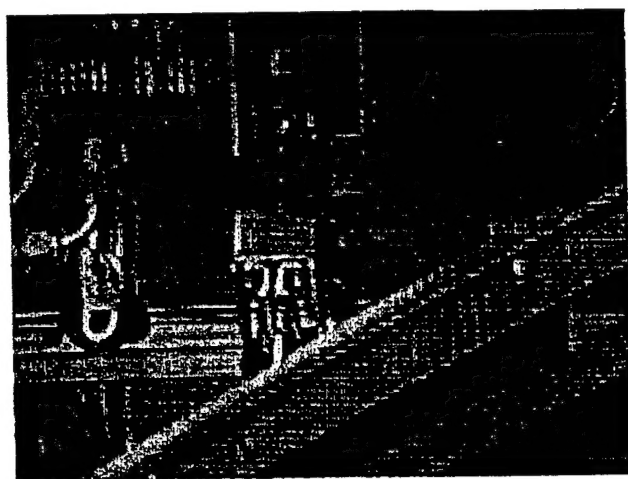


Figure 14. Nozzle Area Prior to G60-P015 Ignition

It was concluded that grain cracking arising from density changes during firing was not wholly responsible for the pressure instabilities associated with solid oxygen test firings.

Another possible explanation for instability was that the grains formed were formed unevenly at the start of the firing. Evidence of this was stumbled upon as the result of an incomplete test in April 1998. The firing (G60-P018) was stopped as a result of a temperature redline after consuming approximately 80% of the grain. Video of the grain chamber during the ensuing purge showed that the remaining oxygen grain was substantially thicker on one side, and already burned through on the other. Figure 15 shows this view; the grain is burned through on the right side. A careful examination of the engine upon disassembly showed that the 'thin' side of the grain corresponded to the area which was most directly exposed to incoming gas from the ignitor. This could have caused the grain non-uniformity in two ways:

- The ignitor flame could have preferentially eroded this surface during the start-up sequence, prior to the onset of the main hydrogen flow. The ignitor burned for approximately 1 second before the main hydrogen was at full flow.
- The freezer gas (oxygen) used to form the grain was plumbed in through the ignitor, and this was where it entered the freezing chamber. Heat transfer from this incoming gas could have caused the grain to be thinner in the area where the gas impinged upon it.

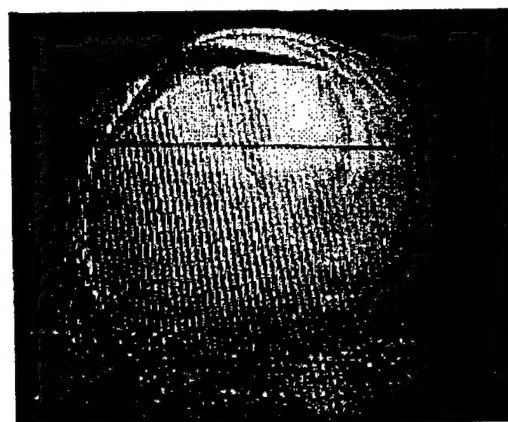


Figure 15. Video of Grain Chamber upon Shutdown of G60-P018

Subsequent calculations revealed that room-temperature oxygen flowing into an 0.2 torr freezing chamber at a flow rate of 6 grams/minute through an entry diameter of 0.3" actually choked to a pressure of around 3 torr (15* chamber pressure) and came blasting into the freezing chamber at near sonic velocity, heating one side of the grain more than the other. This high velocity through an angled entry is expected

to cause significant variations in the convective heat transfer to the wall of the forming solid grain.

All tests performed after G60-P018 brought the freezer gas in through the nozzle, which provided an axisymmetric distribution of freezer gas impinging upon the forming grain. Additionally, all tests after G60-P022 employed a liquid nitrogen pre-chill heat exchanger to cool the incoming GOX to near liquid nitrogen temperatures, further reducing non-uniform heat input from the incoming gas. Video data of the grains formed during these tests provided subjective evidence that the resulting grains were more axisymmetric than previous grains. Figure 16 shows grains from test firings G60-P018 and G60-P019, shortly before the grains were finished freezing. The video camera is located at the head end of the engine, peering down through the SOX grains towards the nozzle. The nozzle throat is visible as the small, black circle in the center. The SOX grains occupy roughly the upper two thirds of the visible area. Note the uniform appearance of the grain from G60-P019; the grain from G60-P018 shows significant waves and ripples, suggesting an uneven surface.



Figure 16. Grains Formed With Non-Axisymmetric (left, G60-P018) and Axisymmetric (right, G60-P019) Freezer Gas Delivery

Figure 17 presents the triple point pressures for hydrogen, oxygen, and methane, along with typical gas flow rates and freezing pressures for these propellants into ORBITEC's cryogenic hybrid freezing chamber. The much higher pressures for methane and hydrogen allowed the freezing to take place at higher pressures, resulting in lower volumetric flow rates of freezer gas and slower entering velocities. These slower rates appear to be one reason for the high degree of uniformity of the solid methane grains, which in turn contributed to the very steady combustion of solid methane that was observed.

Future designs will incorporate new methods of delivering the freezer gas to the freezing surface as uniformly as possible, and as near to the freezing temperature as possible.

Gas	Triple Point Pressure (torr)	Typical Freezing Pressure (torr)	Typical Flow Rate (mole/min)	Pressure/Flow Rate Ratio
O ₂	1.14	0.2	0.2	1
CH ₄	88	80	0.04	2000
H ₂	54	30	0.05	600

Figure 17. Triple Point Pressures and Typical Freezing Pressures and Freezing Flow Rates For Selected Gases

Another possible mechanism which could cause grain irregularities is uneven convective cooling arising from flow of coolant in and out of the coolant bath. However, this is not believed to be a significant factor. This is because the large majority of the thermal resistance is in the solid oxygen grain, not in the convective transfer between the coolant and the engine wall.

In general, grains frozen with freezer gas entering through an axisymmetric path have burned with fewer pressure spikes (see Figures 8, 10, 11). However, there is still much improvement to be made before they reach the desirable 'square wave' appearance.

Potential Use of Ozone

One of the long-term goals of the solid oxygen research is to eventually incorporate a substantial quantity of solid ozone in the oxygen grain. Although ozone has long been recognized as an tremendously energetic oxidizer, the history of attempts to use it in high concentrations as a propellant is replete with disaster because of its tendency for explosive decomposition. Ozone decomposes according to the following chemical reaction:



Pure solid ozone which decomposes to oxygen will produce oxygen gas with a temperature of nearly 2500 K. Calculations show that the theoretical specific impulse for pure ozone/hydrogen systems exceeds that of oxygen/hydrogen by over 40 seconds. If a mixture of solid oxygen/solid ozone could be demonstrated to be a safe propellant, significant performance gains would be possible over current state-of-the-art LOX/LH₂ engines.

Solid Hydrogen Test Firing

One solid hydrogen test firing has been performed by ORBITEC. It was performed on October 25, 1996, with a grain mass of 12 g, a duration of 3 seconds, and a gaseous oxygen flow rate of 3.5 g/sec. The maximum steady pressure obtained was 60 psia. Figure 18 presents the pressure trace for this test firing.

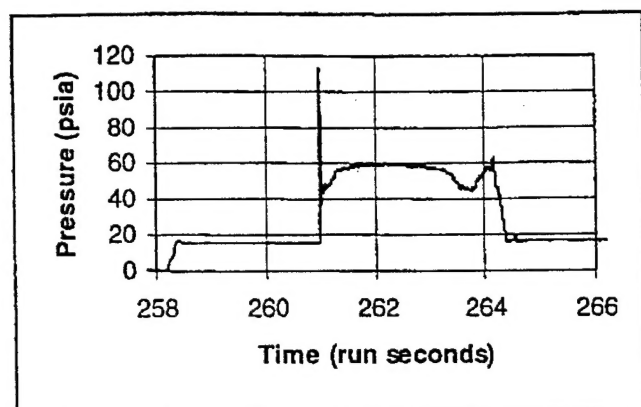


Figure 18. Pressure Trace for SH_2/GO_2 Firing in Mark-II Engine

Regression Rate Summary

The regression characteristics for ORBITEC's cryogenic hybrids are summarized in Figure 19. The vertical axis represents the average regression rate and the horizontal axis is the average oxygen mass flux or, in the case of the solid oxygen hybrids, the average hydrogen mass flux.

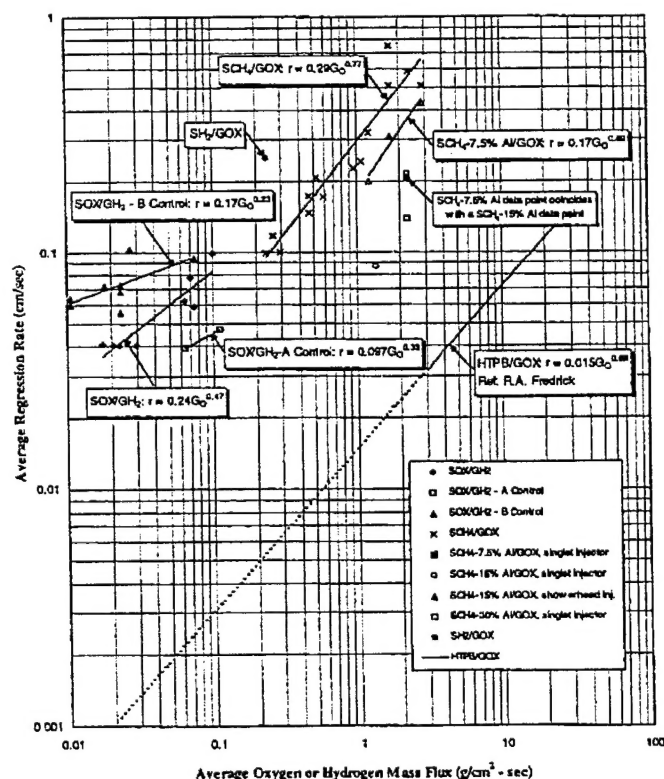


Figure 19. Regression Rate Summary for ORBITEC's Solid Cryogen Hybrid Test Firings

As the graph shows, the most striking trait of these hybrids is that they regress more than an order of magnitude faster than

conventional hybrids (HTPB) for a given port mass flux while still obeying the classical hybrid regression law. These high regression rates reduce the need for complex grain designs and provide increased mass fractions due to the smaller required initial port area. This result coupled with the high combustion performance of these propellants may allow substantial increases in overall hybrid engine efficiencies.

The one solid hydrogen firing resulted in an extremely fuel rich burn. As can be seen in the plot, solid hydrogen regresses the fastest for a given port flux.

Current R&D Activity

ORBITEC's currently sponsored R&D in this area is by the USAF/RL under contract F04611-97-C-0020, titled "Advanced Cryogenic Rocket Engine for Testing High-Energy Propellants". We are currently in design of a scaled-up solid oxygen flight-type engine system which will use liquid hydrogen as the coolant and fuel. The engine will hold an oxygen grain of approximately 10 kg, a scale-up factor of 50 from the current engine. The design is based upon the head end/aft end dual injection concept.

Acknowledgments

Work reported here is from several contract and in-house R&D activities. Contributions and contributors to this work are listed below:

Funded Projects/Organizations:

"Cryogenic Rocket Engine for Testing High-Energy Propellants" USAF Contract F04611-97-C-0020
USAF Research Laboratory, Edwards Air Force Base, CA
COTR Dr. Patrick G. Carrick, OLAC-RL

"Storage and Delivery Device for Solid Oxygen" USAF Contract F04611-93-C-0149
USAF Phillips Laboratory, Edwards Air Force Base, CA
COTR Dr. Patrick G. Carrick, OLAC-PL

"Advanced Cryogenic Hybrid Rocket Engine (ACHRE) for Testing High-Energy Propellants" USAF Contract F04611-96-C-0034
USAF Research Laboratory, Edwards Air Force Base, CA
COTR Dr. Patrick G. Carrick, OLAC-RL

"Metallized Cryogen for Advanced Hybrid Engines (MCHE-II)" NASA Contract NAS3-27382
NASA Lewis Research Center, Cleveland, Ohio
COTR Bryan Palaszewski, NASA/LeRC